Journal of Magnetism and Magnetic Materials 324 (2012) 2011–2018

Contents lists available at SciVerse ScienceDirect

Journal of Magnetism and Magnetic Materials

journal homepage: www.elsevier.com/locate/jmmm

Magnetic, structural, and transport properties at very high temperature in manganites

Fabian Enrique Nima Ramirez, Fabio Furlan Ferreira, Wendel Andrade Alves, José Fernando Queiruga Rey, José Antonio Souza *

Centro de Ciências Naturais e Humanas, Universidade Federal do ABC, Santo André, CEP 09090-400, SP, Brazil

ARTICLE INFO

Article history:
Received 21 December 2011
Available online 10 February 2012

Keywords:
Manganite
Phase transition
Polaron mechanism
Spin-lattice-charge coupling

ABSTRACT

Magnetic, structural, and electric transport measurements at high temperatures were carried out on $La_{1-x}Ca_xMnO_3$; $x=0.20$, 0.25, 0.30, 0.34, 0.40, and 0.45. All samples show a first-order structural phase transition from orthorhombic *Pnma* to rhombohedral $R\bar{3}c$ space group at T_{R-O}. Magnetic susceptibility measurements show that the Curie–Weiss law is strictly obeyed in the rhombohedral phase as opposed to the orthorhombic phase where the effective magnetic moment has a temperature dependence. The electrical resistivity is well described by the small polaron hopping mechanism in the samples up to $x=0.34$. As the charge carriers are introduced into the system ($x=0.40$ and 0.45), this mechanism of hopping ceases to be valid. The value of Grüneisen parameter obtained through analysis of high-resolution X-ray powder diffraction as a function of temperature increases abruptly for the sample with $x=0.40$. This is consistent with an increase in bending and stretchinglike frequency modes observed by Raman spectroscopy.

1. Introduction

The microscopic mechanism underlying electronic, structural, and magnetic properties in strong spin–lattice–charge coupled systems is a subject of great interest in condensed matter physics [1]. The prototypal spin–charge–lattice coupled manganese perovskite $LaMnO_3$ is an antiferromagnetic and insulating system [2,3]. The introduction of holes (Mn^{4+}) into the Mn^{3+} e_g orbitals creates ferromagnetic double exchange interactions which couples the magnetic system with electrical conductivity [4], while Jahn–Teller distorted ions Mn^{3+} couple the magnetic and lattice degrees of freedom. This unusually strong coupling between the electronic, magnetic, and structural properties is suggested to bring about the colossal magnetoresistance effect [5,6]. Once the correlation among degrees of freedom is achieved a better understanding of the thermodynamic quantities of these systems will emerge. However, structural, magnetic, and electrical conductivity studies at very high temperatures in those systems are scarce in the literature. This has led to difficulties in understanding the order parameters and the coupled physical properties of the system.

In general, it is well accepted that the electrical transport mechanism of manganites is well described by the small polaron hopping [7–9]. The localized carriers distort the surrounding lattice exchanging energy and thus forming a bounded polaron. In a simplified approach for manganites, a small lattice polaron can be formed when an e_g electron localizes on a Mn^{3+} ion, and the surrounding oxygen octahedron is distorted due to the Jahn–Teller (JT) effect.

On the other hand, it is not known if there exists a limit at which this model ceases to be valid when charge carriers are varied. Several works have shown that this model fails for some manganite systems, but there is no systematic study revealing the driven physical parameter responsible for deviations from small polaron mechanism [9–14]. Nevertheless, in general those fittings are made at intermediate temperature, close to the ferromagnetic transition, where fluctuations of the clustered magneticlike environment surrounding small polarons influence strongly the electrical transport mechanism [11–14]. In addition, most of the literature is focused on the interplay between magnetic and transport properties, and no systematic study has been made to understand the correlations between the electrical resistivity and crystal structure in the paramagnetic semiconducting state.

In this work, we show that the small polaron hopping mechanism ceases to be valid as charge carriers are introduced into the system. The magnetic results indicate no significantly evidence of direct correlation between the breakdown of transport mechanism and the increase of the effective magnetic moment. Measurements of high-resolution X-ray power diffraction and Raman spectroscopy were put forward to obtain insight on nature of

* Corresponding author.
E-mail address: joseantonio.souza@ufabc.edu.br (J.A. Souza).

0304-8853/$ - see front matter © 2012 Elsevier B.V. All rights reserved.
doi:10.1016/j.jmmm.2012.01.036

charge and lattice correlation. We have observed that such a deviation from small polaron hopping mechanism is consistent with an increase in the Grüneisen parameter. The electrical resistivity value at room temperature is suggested to be related to the abrupt change in the bending and stretching modes as charge carriers are introduced into the system.

2. Experimental

Polycrystalline samples of $La_{1-x}Ca_xMnO_3$ were prepared by sol–gel method. Samples prepared through this chemical route have better chemical homogeneity than when using the standard solid-state reaction method. Stoichiometric amounts of hydrated manganese acetate ($C_4H_6MnO_4 \cdot 4H_2O$) and nitrates of the remaining cations were dissolved in distilled water containing a 50 mol% excess of citric acid and ethylene glycol. The polymeric precursor was formed by heating and stirring the solution at 120 °C. After a few hours a gel is formed, and then dried. The organic material was oxidized 24 h at 600 °C. The powder was ground with an agate mortar for 30 min, heat treated 15 h at 1000 °C. This last step was repeated three times with reaction temperatures of 1050 °C, 1100 °C and 1300 °C. Finally, the powder was ground for 30 min, pressed into pellets and reacted 40 h at 1350 °C. The density of our samples is very high approximately 97% of theoretical density. The X-ray powder diffraction indicates that all samples are single phase belonging to orthorhombic space group *Pnma*. The average Mn oxidation state was determined by iodometric titration. The titration procedure was repeated at least three times for each sample. The titration experiment determines the average Mn valence under the assumption that the valences of La, Ca, and O are +3, +2, and −2. It is well known that these Mn oxides possess La and Mn defects rather than an oxygen excess. The obtained average Mn valence was 3.23(1), 3.27(1), 3.32(1), 3.35(1), 3.42(1), 3.46(1) for $x=0.20$, 0.25, 0.30, 0.34, 0.40, and 0.45, respectively. Magnetization measurements (from 10 K to 900 K) were performed using a standard vibrating sample magnetometer (VSM) oven option from Quantum Design. Electrical resistivity was measured using a four-probe method using a home-made apparatus with a platinum thermometer mounted close to the sample. Silver epoxy was used to make contacts to the sample. Data were collected in air on warming to the highest temperature followed by cooling. We have performed both thermogravimetric analysis (TGA) and differential scanning calorimetry (DSC) up to 950 K (not shown). DSC shows a robust peak indicating a phase transition for the samples and TGA revealed no changes in the studied temperature range, indicating negligible oxygen loss. High-resolution X-ray powder-diffraction (HRXPD) measurements were conducted on the XPD beamline at the Laboratório Nacional de Luz Síncrotron [15]. The sintered pellet was ground and sieved to reject grains larger than ~5 μm. Wavelength of 1.240 and 2θ steps of 0.005° were chosen for our measurements. A furnace with Ar flow was employed for the high-temperature measurements. Raman spectra were recorded in a Renishaw Raman System 3000 spectrometer, with a CCD detector, coupled to an Olympus BTH2 microscope (80-fold enhancement). A He–Ne laser (Spectra Physic, model 127) with excitation radiation at 632.8 nm, was used.

3. Results and discussion

In Fig. 1 the electrical resistivity as a function of temperature is presented for all samples studied herein, $x=0.20$, 0.25, 0.30, 0.34, 0.40, and 0.45. A thermally activated electrical transport mechanism—semiconductinglike behavior is clearly observed for

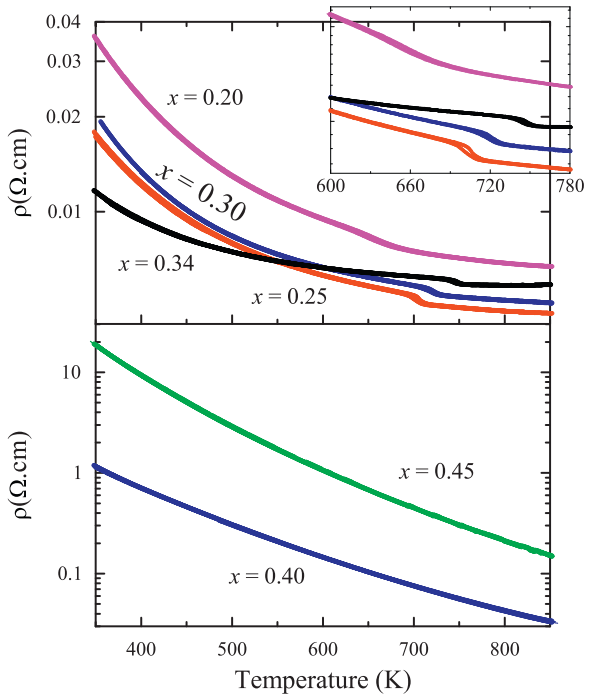

Fig. 1. Electrical resistivity as a function of temperature for $La_{1-x}Ca_xMnO_3$, $x=0.20$, 0.25, 0.30, 0.34, 0.40, and 0.45. The inset shows a thermal hysteresis in the samples with $x=0.20$, 0.25, 0.30, and 0.34 due to a structural phase transition from orthorhombic (O) to rhombohedral (R) space group.

all samples. It is known that this family $La_{1-x}Ca_xMnO_3$ shows an orthorhombic to rhombohedral structural phase transition T_{R-O} at high temperatures [16]. In samples with $x=0.20$, 0.25, 0.30, and 0.34, this structural phase transition brings about a hysteretic behavior at T_{R-O} revealing the first order nature of the transition. Interestingly, neither a hysteretic behavior nor any feature is detected in samples with $x=0.40$ and 0.45 by the electrical resistivity measurements. As we shall see in the unit-cell parameters obtained by high-resolution X-ray diffraction data the sample with $x=0.45$ also undergoes a structural phase transition, even though not visible by the electrical resistivity data. Furthermore, it is observed that as charge carriers are introduced into the system, the electrical resistivity decreases and abruptly increases above $x=0.40$. The value measured in the samples with $x=0.20$, 0.25, 0.30, and 0.34 is in the range of 0.01−0.04 Ω cm, while in the samples with $x=0.40$ and 0.45 it is in the range of 1−20 Ω cm. The magnitude of the electrical resistivity close to T_{R-O} in samples $x=0.20$, 0.25, 0.30 and 0.34 has the same order (5 mΩ cm) as that found in manganites with bad metal behavior [17], suggesting a more delocalized character of the charge carriers.

The electrical resistivity in the small polaron model may be expressed as [7,18]

$$\rho(T) = AT^s \exp(E_p/k_BT) \quad (1)$$

where A is a pre-factor, E_p is the polaron activation energy, and k_B is the Boltzmann constant. In the adiabatic regime $s=1$ (non-adiabatic regime $s=3/2$), the hopping of electrons is faster (slower) than the vibration of the optical phonon mode [7,8,19].

In Fig. 2, we plot the data assuming both adiabatic and nonadiabatic regimes for samples with $x=0.20$, 0.25, 0.30, and 0.34. As can be observed, all samples may be fitted using those regimes in both rhombohedral and orthorhombic phases. In a previous work, Souza et al. [19] showed that a temperature dependence of electrical resistivity in high temperatures for $x=0.30$ can be explained by the small polaron hopping mechanism. They observed a subtle change from adiabatic to nonadiabatic